Development 130, 2589-2601

doi:10.1242/dev.00500

The *C. elegans* LIM homeobox gene *lin-11* specifies multiple cell fates during vulval development

Bhagwati P. Gupta, Minqin Wang* and Paul W. Sternberg†

HHMI and Division of Biology, California Institute of Technology, Pasadena, CA 91125, USA
*Present address: University of Illinois College of Law, Champaign, IL 61820, USA
†Author for correspondence (e-mail: pws@caltech.edu)

Accepted 17 March 2003

SUMMARY

LIM homeobox family members regulate a variety of cell fate choices during animal development. In *C. elegans*, mutations in the LIM homeobox gene *lin-11* have previously been shown to alter the cell division pattern of a subset of the 2° lineage vulval cells. We demonstrate multiple functions of *lin-11* during vulval development. We examined the fate of vulval cells in *lin-11* mutant animals using five cellular markers and found that *lin-11* is necessary for the patterning of both 1° and 2° lineage cells. In the absence of *lin-11* function, vulval cells fail to acquire correct identity and inappropriately fuse with each other. The expression pattern of *lin-11* reveals dynamic changes during development. Using a temporally controlled overexpression system, we show that *lin-11* is initially required in vulval cells for establishing the correct invagination pattern. This process involves asymmetric expression of *lin-11* in the 2° lineage cells. Using a conditional RNAi approach, we show that *lin-11* regulates vulval morphogenesis. Finally, we show that LDB-1, a NLI/Ldb1/CLIM2 family member, interacts physically with LIN-11, and is necessary for vulval morphogenesis. Together, these findings demonstrate that temporal regulation of *lin-11* is crucial for the wild-type vulval patterning.

Key words: *C. elegans*, *lin-11*, *ldb-1*, LIM homeodomain, Vulva, Differentiation

INTRODUCTION

Specification of different cell types during development involves multiple cell-cell interactions mediated by many genes. Studies of the *C. elegans* hermaphrodite vulva have proven successful in dissecting regulatory networks and understanding the function of some crucial genes. The adult vulva is formed by the progeny of three out of six vulval precursor cells (VPCs) that acquire 1° and 2° fates in a 2°-1°-2° pattern, and undergo three rounds of cell divisions (Sulston and Horvitz, 1977) (Fig. 1). During L4 stage, vulval cells differentiate into seven different cell types and form an invaginated structure (Sharma-Kishore et al., 1999) (Fig. 1). Vulval development thus provides opportunities to study cell-fate specification and pattern formation. Mutations that perturb vulval morphology have identified some of the genes that regulate cell differentiation, including *lin-17* (*frizzled* family), *lin-18* and *lin-11* (LIM homeobox family) (Ferguson and Horvitz, 1985; Ferguson et al., 1987; Freyd et al., 1990; Sawa et al., 1996; Gupta and Sternberg, 2002). Mutations in these genes alter the axes of terminal cell division, suggesting a role in differentiation of a subset of the vulval cells. *lin-11* is known to be necessary for the NT portion of the 2° lineage vulval cells because there is a LLLL cell lineage pattern in *lin-11* mutant animals compared with the wild-type NTLL pattern (see Fig. 1) (Ferguson et al., 1987). Being a LIM homeodomain family member, LIN-11 is likely to function as a transcriptional regulator of vulval cell-type specific genes.

The LIM homeodomain proteins have two LIM domains and a homeodomain (reviewed by Hobert and Westphal, 2000; Bach, 2000). The LIM domains are thought to mediate protein-protein interactions and regulate tissue-specific function. *Drosophila* Apterous is required for specifying the dorsal region of the wing imaginal disc (Cohen et al., 1992; Diaz-Benjumea and Cohen, 1993). Isl1 was identified for its role in the development of pancreatic endocrine cells (Karlsson et al., 1990) and subsequently found to be involved in the formation of motor- and interneurons and pituitary cells (Pfaff et al., 1996; Takuma et al., 1998). Lhx2 is involved in the development of eye, forebrain, erythrocytes and limbs (Porter et al., 1997; Rodriguez-Esteban et al., 1998). Mutations in human *LMX1B* cause ‘nail patella syndrome’ owing to defects in specification of the patellar mesenchyme of the dorsal limbs (Dreyer et al., 1998; Vollrath et al., 1998).

The *C. elegans* genome encodes seven LIM homeodomain proteins including LIN-11 (Ruvkun and Hobert, 1998). LIN-11 has been shown to be necessary for the development of a subset of vulval cells, uterine π lineage cells and some neurons (Ferguson et al., 1987; Hobert et al., 1998; Newman et al., 1999; Sarafi-Reinach et al., 2001; Gupta and Sternberg, 2002). In this study, we show that the spatiotemporal expression of *lin-11* confers distinct cell fates. Our experiments reveal at least

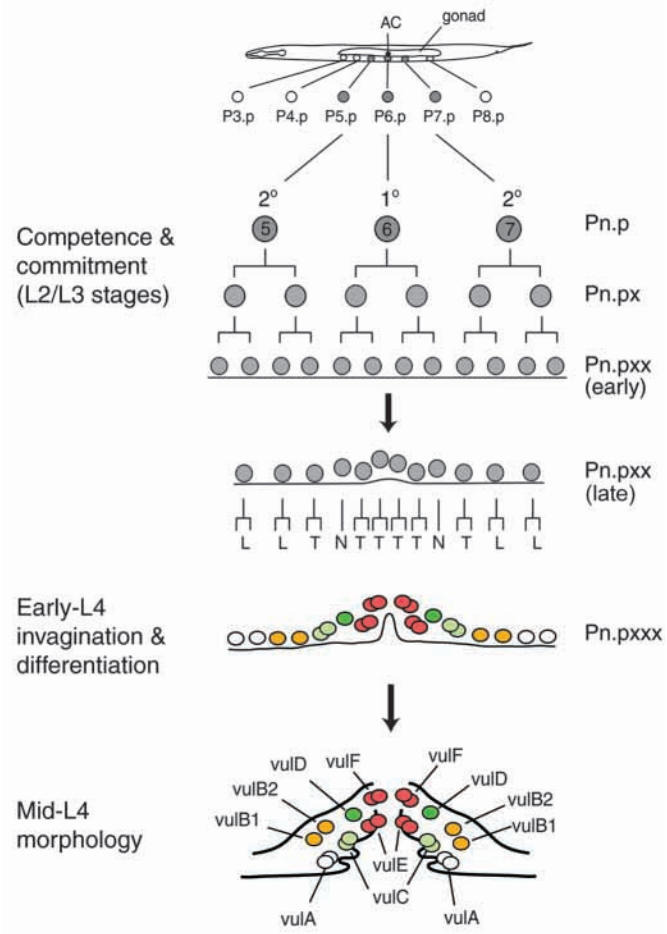

Fig. 1. Wild-type vulval development. During L2/L3 stages, the anchor cell (AC) induces P5.p, P6.p and P7.p VPCs to adopt 1° and 2° cell fates. The relative positions of the cell nuclei have been drawn. The terminal cell division axes are NTLL for the 2° lineage and TTTT for the 1° lineage (N, not divided; T, transverse; L, longitudinal). The Pn.pxxx cells invaginate during L4 stage to give rise to the future vulval opening. The seven differentiated cell types have been marked with colors (1° lineage vulE and vulF are red; 2° lineage vulA are white; vulB1 and vulB2 are yellow; vulC are light green; and vulD are dark green).

two distinct functions of *lin-11* in vulval cells. *lin-11* is first required for setting up the correct pattern of vulval invagination. During this phase, the precursors of vulC and vulD express high levels of *lin-11*. Later on, *lin-11* is expressed in all vulval progeny. Using a conditional RNAi approach, we have examined *lin-11* function during vulval morphogenesis and demonstrate that *lin-11* is required in vulval progeny for wild-type patterning. Finally, we show that the LIM-binding protein LDB-1 (Cassata et al., 2000) plays a role in vulval differentiation by directly interacting with LIN-11.

MATERIALS AND METHODS

Strains and culture conditions

C. elegans were grown and mutagenized according to published methods (Brenner, 1974; Wood, 1988). Except for the heat shock strains, for which a 15°C incubator was used, all other strains were maintained at 20°C. Mutations and transgenes used are as follows.

LGI: *lin-11(n389)* and *lin-11(n566)* (Ferguson and Horvitz, 1985), and *ayIs4*[*egl-17::GFP* + *dpy-20*(+)] (Burdine et al., 1998)

LGII: *syIs54*[*ceh-2::GFP* + *unc-119*(+)]

LGIII: *syIs80*[*lin-11::GFP* + *unc-119*(+)] (Gupta and Sternberg, 2002)

LGIV: *dpy-20(e1282)* (Brenner, 1974), *syIs49*[*zmp-1::GFP* + *dpy-20*(+)] (Wang and Sternberg, 2000)

LGV: *nIs96*[*lin-11::GFP* + *lin-15*(+)] (Reddien et al., 2001), *syIs53*[*lin-11::GFP* + *unc-119*(+)] (Gupta and Sternberg, 2002)

LGX: *syIs50*[*cdh-3::GFP* + *dpy-20*(+)]

Other transgenic strains include *syIs78*[*ajm-1::GFP* + *unc-119*(+)], *syEx500*[*pPHS11.82(hs::lin-11)* + *pTG96(sur-5::GFP)*], *syEx530*-[*pPHS11.82(hs::lin-11)* + *myo-2::GFP*], *syEx552*[*pPHS11.12(hs::lin-11)* + *pPHS11.12i(hs::lin-11i)* + *myo-2::GFP* + *unc-119*(+)], *syEx551*[*pLBP13.3c(ldb-1::GFP)*] and *syEx565*[*unc-119*(+) + *pLBP13.3c(ldb-1::GFP)*]. Stably transmitting extrachromosomal array lines and integrants were generated by standard techniques (Mello et al., 1991; Way et al., 1991).

Microscopy and laser ablations

Vulval cells and lineages were examined using Nomarski optics (see Wood, 1988). *GFP* expression was examined using a Zeiss Axioplan microscope equipped with a GFP filter HQ485LP (Chroma Technology), a power source (Optiquip 1500) and a 200 W OSRAM Mercury bulb.

Laser ablations were performed as described by Avery and Horvitz (Avery and Horvitz, 1987). Early- to mid-L3 stage worms were chosen for the study.

Heat-shock experiments

hs::lin-11 animals (*syEx500* and *syEx530*) were pulsed at different temperatures (between 30°C to 33.5°C) and duration (15 minutes to 1 hour) during Pn.px and Pn.pxx stages. In general, stronger pulses (1 hour at 31°C or 30 minutes at 33.5°C) caused growth arrest, uncoordinated movement and larval lethality. These are probably the result of interference with the function of other LIM homeobox genes (Ruvkun and Hobert, 1998). Alternatively, high levels of *lin-11* expression in neurons may interfere with their normal development (Hobert et al., 1998; Sarafi-Reinach et al., 2001). For the vulval phenotypes, we used a 20 minutes heat shock at 33°C.

lin-11 RNAi animals (*hs-dslin-11i*) were heat shocked during early Pn.pxxx stage for 1 hour at 33°C. After recovery at 20°C, vulval phenotypes were examined during mid-L4 stage.

Molecular biology

hs::lin-11 construct (pPHS11.82)

To construct pPHS11.82, a 1.5 kb *Nsi*I-*Kpn*I *lin-11* genomic fragment from the cosmid ZC247 was cloned into pPD49.83 (Mello and Fire, 1995). As the construction deleted 125 bp of the *hsp16-41* promoter, it was restored as a *Nsi*I fragment by PCR amplification of the vector DNA using primers FBG3 (5′CGGCTCGTATGTT-GTGTGGAATTG3′) and BBG2 (5′CGCGATGCATGATGAGG-ATTTTCGAAGTTTTTTAG3′). The resulting construct was digested with *Sph*I and *Kpn*I to obtain a 1.9 kb DNA fragment. In a separate experiment, a 10.8 kb ZC247 *Nco*I fragment was inserted in pPD49.83 to obtain pPHS11.108. pPHS11.108 was digested with *Sph*I and *Kpn*I and subsequently ligated with the 1.9 kb *Sph*I-*Kpn*I fragment to obtain pPHS11.82. The beginning and end sequences (18 nucleotides) of the *lin-11* genomic fragment are 5′-ATGCATTCTTCTTCTTCG-3′ and 5′-CCATGGTTCCTATGAGGT-3′.

lin-11 RNAi constructs

To construct *lin-11* RNAi plasmids, *lin-11* cDNA (yk452f7; kindly provided by Dr Yuji Kohara, National Institute of Genetics) was separately cloned in sense (pPHS11.12) and antisense (pPHS11.12i) orientations into pPD49.83 (see Gupta and Sternberg, 2002).

ldb-1::GFP construct (pLBP13.3c)

The cosmid F58A3 was digested with *Sph*I and *Pst*I and a 13.3 kb fragment was subcloned into pPD95.73 (a gift of A. Fire, S. Xu, J. Ahnn and G. Seydoux). The beginning and end sequences (18 nucleotides) of the fragment are: 5′-GCATGC-TTTTTTTTAATT-3′ and 5′-CTGCAGCTGTAGCTTTTT-3′.

ldb-1 RNAi construct (pYK66F4-1)

ldb-1 cDNA (yk66f4, kindly provided by Dr Yuji Kohara, National Institute of Genetics) was digested with *EcoR*I and *Not*I and a 720 bp fragment was subcloned in pBS-SK(+). In vitro RNA was synthesized using the Ambion MEGAscript kit.

ldb-1 RNAi experiments

ldb-1 RNAi was performed by soaking (Tabara et al., 1998). An equal amount of each RNA strand (20 μl) was mixed to generate dsRNA. For control RNA, the pBS-SK(+) vector with no *ldb-1* insert was used. Worms were synchronized by 24 hours L1 starvation in M9 after bleach treatment of the adult hermaphrodites. A small aliquot of the L1 stage worms was mixed with dsRNA solution (5 to 20 μl) and 1-5 μl OP50 bacteria. Worms were incubated for 30-36 hours, at which time they were washed twice with M9 and transferred to regular plates seeded with OP50. L4 stage animals were examined for the vulval phenotype and *GFP* expression.

Two-hybrid experiments

Two-hybrid experiments were performed as suggested by the manufacturer (Clontech/BD Biosciences). pGBKT7 (*GAL4* DNA binding) and pGADT7 (*GAL4* activation) vectors were used to subclone *lin-11* and *ldb-1* cDNA fragments, respectively. Positive control vectors were pVA3 (murine p53 insert) and pTD1 (SV40 large T-antigen insert). To subclone *lin-11* LIM domains, a 682 bp product was PCR amplified using primers lin-11-LIM-u1 (5′GGCATATGACCTCACTGGAAGAAGAGGAG3′) and lin-11-LIM-d1 (5′GGGTCGACTCGAGTCATCTGAATTGTCCTTC3′) and *lin-11* cDNA as a template. The resulting product was digested with *Nde*I and *Sal*I and subcloned in pGBKT7. *ldb-1* LID region (553 bp) was PCR amplified using primers ldb-1-LID-u1 (5′GGCA-TATGGGAAGCAAAAAAGCTACAGCTG3′) and ldb-1-LID-d1 (5′GGCTCGAGGTGGCATCCGACTATTCGGCATC3′) and the template *ldb-1* cDNA. PCR product was digested with *Nde*I and *Xho*I and subcloned in pGADT7. Transformed AH109 yeast cells were grown on SD/–Leu/–Trp and SD/–His/–Leu/–Trp plates at 30°C.

RESULTS

lin-11 mutant vulval cells exhibit abnormal cell fusions

Previous studies of *lin-11* function during vulval development have defined its requirements during differentiation of a subset of the vulval progeny: vulC and vulD (Ferguson et al., 1987). Two experiments suggested that *lin-11* might be involved in patterning additional vulval cells. First, in a screen for mutants with altered patterns of *egl-17::GFP* and *ceh-2::GFP* expression, three *lin-11* alleles *(sy533, sy534* and *sy634)* were recovered. Second, ablation of the daughters of P5.p and P7.p VPCs in *lin-11* mutant animals did not alter the invagination defect of P6.p progeny, suggesting that the effects on 1° lineage are not an indirect consequence of the 2° lineage defect. To analyze the defects in *lin-11* mutant vulval cells further, we used the *ajm-1::GFP* cell-junction marker (formerly known as *MH27::GFP* and *jam-1::GFP*) that reveals cell boundaries and allows the in vivo study of cell fusion events (Podbilewicz and White, 1994; Mohler et al., 1998; Raich et al., 1999). Sharma-Kishore et al. have used the marker to describe the process of wild-type vulval development (Sharma-Kishore et al., 1999).

We examined *ajm-1::GFP* vulval expression in mid-L4 stage animals. Fig. 2A shows a typical wild-type expression (ventral view) in the form of seven concentric rings that arise from specific fusion between vulval cells (Sharma-Kishore et al., 1999). These rings are visible at different focal planes since vulval cells have invaginated significantly (see Fig. 2B for a schematic representation). Each of the vulval rings represents one cell type (vulA-vulF; Fig. 2B). By contrast, *ajm-1::GFP* expression in *lin-11(n389)* animals reveals dramatic defects in cell fusion events. In all 12 animals examined, only two or three vulval rings could be seen; moreover, the rings were visible in the same focal plane (Fig. 2C,D,F,G). One of these rings was unusually large (big arrowheads in Fig. 2C,D) and encircled one or two smaller odd-shaped rings (small arrows in Fig. 2C,D). The big ring corresponds to the P5.p and P7.p progeny that have fused together, while the smaller ones belong to the P6.p progeny. In 30% of these animals some of the 2° lineage cells did not fuse with the large syncytium and remained isolated (red star brackets in Fig. 2C,F). Some of these cells (two to six) showed punctate *ajm-1::GFP* expression, suggesting partial fusion with the surrounding hyp7 syncytium (Fig. 2C). To confirm that the large syncytium is 2° lineage specific, we ablated the P6.p progeny during early L3 stage and found no change in the formation of large syncytium (*n*=4; Fig. 2E).

We also observed defects in *ajm-1::GFP* expression in the 1° lineage vulval cells. In these cases, the defect appeared to be the smaller size of the vulE and vulF rings, and their failure to align correctly (small arrows in Fig. 2C,D). To determine whether the 1° lineage defect is due to the autonomous requirement of *lin-11*, we ablated P5.p and P7.p cells during early L3 stage. Such ablated animals still showed morphological defects in vulE and vulF rings (*n*=3, Fig. 2H). Together, these results provide strong evidence that *lin-11* is necessary for the development of all 1° and 2° lineage vulval cells. We did not observe any cell fusion defect in *lin-11(n389)* animals at the earlier stages of vulval development.

lin-11 mutant vulval cells fail to acquire correct identities

To study the properties of developing vulval cells in *lin-11* mutant animals further, we examined cell-type specific markers that are expressed in overlapping subsets of vulval cells. These include *egl-17* (fibroblast growth factor receptor homolog), *cdh-3* (cadherin family), *zmp-1* (zinc metalloprotease) and *ceh-2* (homeobox family) (Pettitt et al., 1996; Burdine et al., 1998; Wang and Sternberg, 2000; Inoue et al., 2002).

egl-17 expression in vulval cells has been shown to be a faithful marker of wild-type development (Burdine et al., 1998; Ambros, 1999; Wang and Sternberg, 1999). The earliest expression of *egl-17::GFP* is detected in P6.p. The expression continues in the P6.p lineage during Pn.px (VPC progeny after first cell division, x denotes both anterior and posterior cells) and Pn.pxx (VPC progeny after second cell division) stages. However, after third cell division of VPCs (Pn.pxxx cells) *egl-17::GFP* expression is no longer detected in the P6.p lineage but instead is expressed in the vulC and vulD progeny of the 2° lineages (Burdine et al., 1998) (Fig. 3A,B). We find that

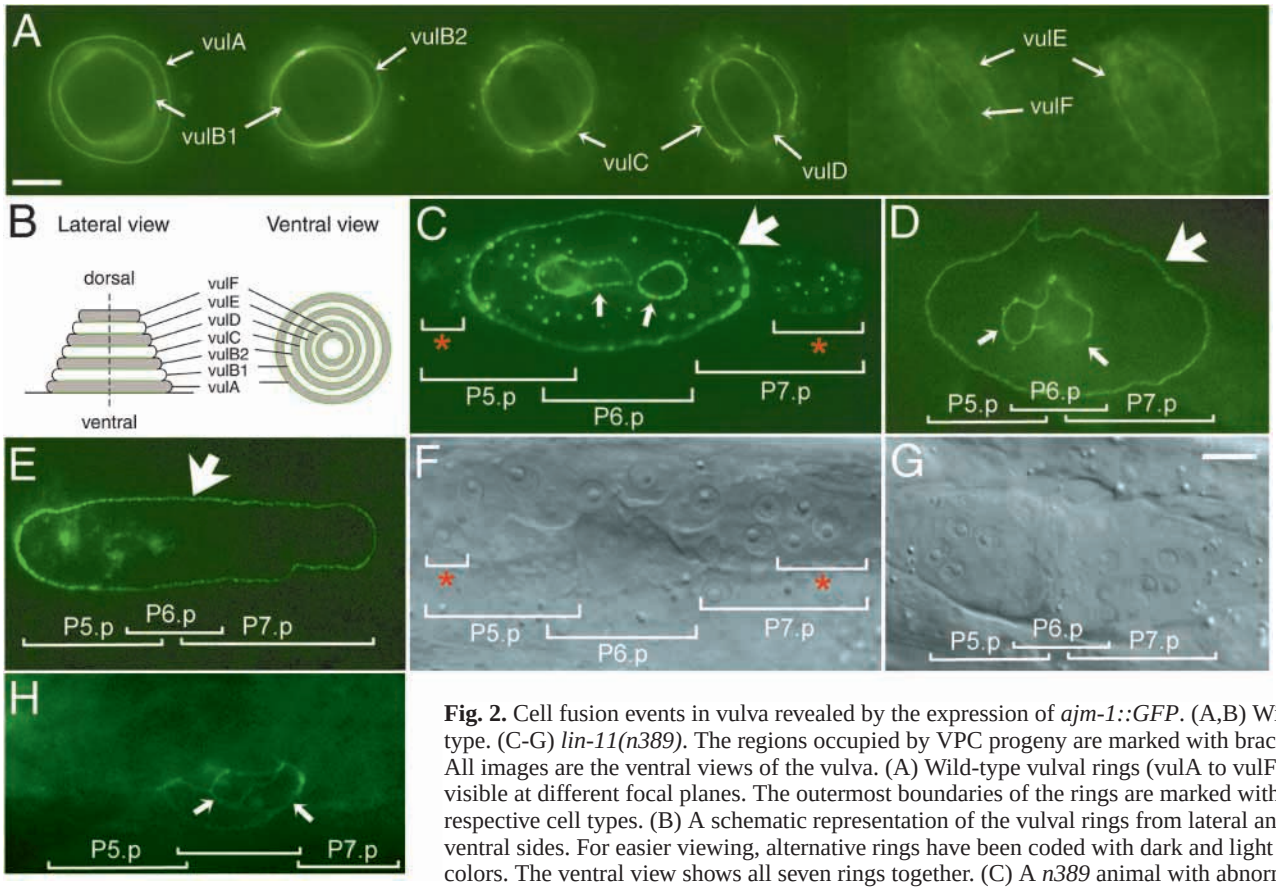

Fig. 2. Cell fusion events in vulva revealed by the expression of *ajm-1::GFP*. (A,B) Wild-type. (C-G) *lin-11(n389)*. The regions occupied by VPC progeny are marked with brackets. All images are the ventral views of the vulva. (A) Wild-type vulval rings (vulA to vulF) are visible at different focal planes. The outermost boundaries of the rings are marked with respective cell types. (B) A schematic representation of the vulval rings from lateral and ventral sides. For easier viewing, alternative rings have been coded with dark and light colors. The ventral view shows all seven rings together. (C) A *n389* animal with abnormal vulval fusions. The outermost ring (big arrow) corresponds to the 2° lineage cells. The inside rings (small arrows) belong to the 1° lineage cells. Brackets marked with red star point to the unfused vulval cells (punctate GFP). (F) Same animal as in C, under Nomarski. (D) Another *n389* animal. In this case, all 2° lineage cells have fused together (big arrow). The small arrows point to the 1° lineage rings. (G) Same animal as in D, under Nomarski. (E) P6.p lineage cells were ablated in this *n389* animal. The outermost big ring is still visible (arrow). (H) *n389* animal. P5.p and P7.p lineage cells were ablated during early L3 stage. Vulval rings corresponding to the 1° lineage cells (arrows) have abnormal morphology. Scale bars: in A, 12 μm; in G, 10 μm for C-H.

early expression of *egl-17::GFP* in P6.p lineage is not altered in *lin-11(n389)* animals. However, during the Pn.pxxx stage, the 2° lineage cells fail to express a detectable level of *GFP* (Burdine et al., 1998) (Fig. 3C,D; Table 1). However, the P6.p lineage cells continue to express low levels of *GFP*, suggesting a defect in their differentiation (Fig. 3C,D). Thus, vulC, vulD cells (2° lineage) and vulE, vulF cells (1° lineage) have not acquired the correct identity.

cdh-3 belongs to a cadherin superfamily of genes, members of which are known to play various roles in epithelial morphogenesis such as cellular adhesion and cell shape changes (Gumbiner, 1996; Pettitt et al., 1996; Costa et al., 1998; Hill et al., 2001). The wild-type *cdh-3::GFP* (*syIs50*) expression in vulval cells is detected during L4 stage in the vulC, vulD, vulE and vulF cells (Fig. 3E,F; Table 1). In *lin-11(n389)* animals, *cdh-3::GFP* expression is completely abolished in the presumptive vulC and vulD cells (Fig. 3G,H; Table 1). In addition, expression in the 1° lineage cells is considerably affected: presumptive vulF shows very weak GFP fluorescence, whereas vulE shows fluorescence only on rare occasions (Fig. 3G,H; Table 1). Thus, *lin-11* is required for the differentiation of the vulC, vulD, vulE and vulF cell types.

The *zmp-1* gene encodes a zinc metalloprotease and has been used as a marker for the 1° lineage cells (Wang and Sternberg, 2000; Inoue et al., 2002). *zmp-1::GFP* (*syIs49*) expression in the vulva begins during the late-L4 stage, first detected in the vulD and vulE and later on in the vulA as well (Fig. 3I,J; Table 1) (Wang and Sternberg, 2000; Inoue et al., 2002). We did not find any *zmp-1::GFP* expression in *lin-11(n389)* vulval cells (Fig. 3K,L; Table 1). Thus, *lin-11* is also necessary for the development of the vulA cell type.

We also examined the expression of a homeodomain family member, *ceh-2*, which is expressed during L4 stage in the vulB1, vulB2 and vulC cells (*syIs54*) (Inoue et al., 2002) (Table 1). In *lin-11(n389)* animals, vulval cells failed to express *ceh-2::GFP* in any of the cell types (Table 1).

The defects in vulval markers expression and cell fusion in *lin-11* mutant animals reveal requirements of *lin-11* in the specification of both 1° and 2° lineage cells. It is possible that *lin-11* functions non-autonomously to specify some of the cell fates. To address this possibility, we carried out cell ablation experiments in wild-type and *lin-11(n389)* animals. We ablated a subset of the vulval cells during Pn.px and Pn.pxx stages, and examined expression of four GFP markers (*egl-17::GFP*, *zmp-1::GFP*, *cdh-3::GFP* and *ceh-2::GFP*) in

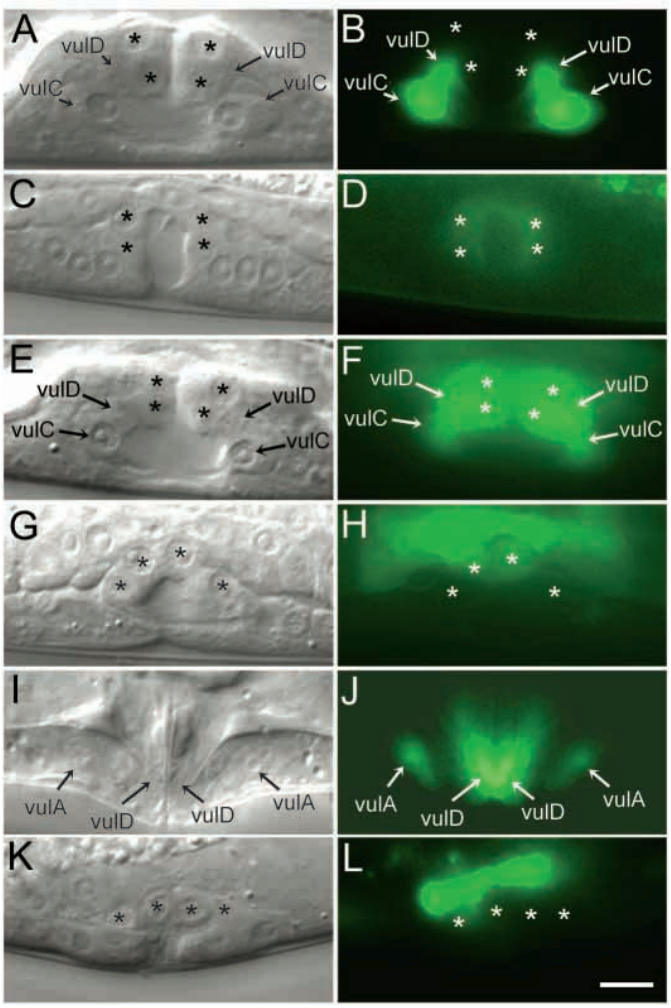

Fig. 3. Expression pattern of the vulval markers in wild-type and *lin-11(n389)* vulva. (A,C,E,G,I,K) Nomarski images of the L4 stage vulval cells. (B,D,F,H,J,L) Corresponding images showing GFP fluorescence. Primary lineage cells have been marked with stars and 2° lineage cells with arrows. Anterior is towards the left. (A,B) Wild-type *egl-17::GFP* expression in the vulC and vulD cells. (C,D) In *n389* background presumptive vulC and vulD do not reveal any *egl-17::GFP*. Instead, weak *egl-17::GFP* is expressed in all the 1° lineage cells. (E,F) Wild-type *cdh-3::GFP* expression is detected in all the 1° lineage cells and in the vulC, vulD of the 2° lineage cells. (G,H) *n389*; *cdh-3::GFP* animals have no detectable GFP fluorescence in the 2° lineage cells. In this animal, the presumptive vulF cells are expressing weak *GFP*, whereas vulE reveal no detectable expression. (I,J) Wild-type *zmp-1::GFP* expression is seen in the vulA and vulD of the 2° lineage. By contrast, *n389*; *zmp-1::GFP* animals (K,L) do not express *GFP* in any of the vulval cells. The bright fluorescence is seen in some uterine lineage cells. Scale bar: 8 μm.

the progeny of the remaining cells during L4 stage (Table 1). Four different ablation sets were analyzed [Set 1 (vulA, B1 and B2), Set 2 (vulC and D), Set 3 (vulA, B1, B2, C and D) and Set 4 (VulE and F)]. We found that in wild-type control animals, all four GFP markers are expressed in cell-autonomous manner, i.e. ablation of a subset of the vulval cells did not alter *GFP* expression pattern in the progeny of the remaining cells (compare intact and cell ablated animals in Table 1). A similar conclusion for the *zmp-1::GFP* was drawn earlier by Wang and Sternberg (Wang and Sternberg, 2000). Having examined the autonomy of the GFP markers in wild-type animals, we carried out similar sets of cell ablations in *lin-11(n389)* animals. The results, summarized in Table 1, demonstrate that *lin-11* functions in all vulval cells and specifies their fate in cell-autonomous manner. We can not rule out the possibility of complex interactions. The cell fusion defects are likely to be a secondary consequence of defects in cell fate specification.

lin-11 is dynamically expressed during vulval development

Our analyses have revealed broader requirements for *lin-11* during vulval development. The vulval expression of *lin-11* using *lin-11::lacZ* reporter assays was previously reported to be in the N and T cells of the 2° lineages (precursors of vulC and vulD) (G. A. Freyd, PhD thesis, Massachusetts Institute of Technology, 1991) (Struhl et al., 1993). This pattern of expression did not provide a suitable explanation for our observations on the *lin-11* mutant phenotypes. To determine the spatial and temporal pattern of *lin-11* vulval expression precisely, we generated several *lin-11::GFP* transgenic lines (Gupta and Sternberg, 2002). Two of these, *syIs80* and *syIs53*, were chosen for detailed analysis. Another *lin-11::GFP* integrant, *nIs96* (Reddien et al., 2001), was also analyzed. The developmental profile of the *lin-11::GFP* vulval expression in all three lines is nearly identical, although their fluorescence brightness can be ranked *nIs96>syIs80>syIs53*. The *syIs80* and *syIs53* animals reveal dynamic changes in the vulval *GFP* expression.

The earliest *GFP* expression in *syIs80* vulval cells is detected in one of the two daughters of the 2° lineage precursors (P5.pp and P7.pa cells) (Fig. 4A,B, Fig. 5A). In most cases, GFP fluorescence was detectable only ~1-2 hours before the VPC daughters were beginning to divide. At this stage, expression in P6.p daughters is much weaker and rarely observed (Fig. 5A). During the Pn.pxx stage, vulval cells begin to reveal brighter GFP fluorescence in both the 1° and 2° lineages (Fig. 4C,D, Fig. 5B). In the 2° lineage, expression is typically seen in only the N and T cells (Fig. 5B). By the Pn.pxxx stage, *lin-11::GFP* expression is detected in all 2° lineage progeny (Fig. 4E,F, Fig. 5C). In general, vulA has the lowest level of expression compared with others. *syIs53* animals reveal a similar pattern of expression, although the overall fluorescence is considerably reduced (compare Fig. 5D with 5B, and Fig. 5E with 5C). The expression of *lin-11* in vulval cells is consistent with the cell fusion defects and marker gene expression studies in *lin-11* mutant animals. Together, these results further support the hypothesis that *lin-11* plays a role in the development of all vulval cell types.

By mid-L4 stage, the GFP fluorescence in *syIs53* and *syIs80* strains begins to fade, and can not be seen by late-L4 stage. However, in *nIs96* animals fluorescence can be detected in young adult animals. Expression is also detected in the uterine π lineage cells, VC neurons and a subset of the head and tail neurons in a manner similar to that reported earlier (Hobert et al., 1998; Newman et al., 1999). In addition, we observe expression in the B.pap and its descendents in the developing male proctodeum.

Table 1. Cell-autonomous expression of vulval markers in wild-type and *lin-11(n389)* animals

		P5.p					P6.p				P7.p					
Marker	*lin-11* locus	A	B1	B2	C	D	E	F	F	E	D	C	B2	B1	A	*n*
ayIs4	+	0	0	0	100	100	0	0	0	0	100	100	0	0	0	47
	n389	0	0	0	0	0	100*	100*	100*	100*	0	0	0	0	0	53
	+	×	×	×	100	100	0	0	0	0	100	100	×	×	×	10
	n389	×	×	×	0	0	100*	100*	100*	100*	0	0	×	×	×	11
	+	0	0	0	×	×	0	0	0	0	×	×	0	0	0	6
	n389	0	0	0	×	×	100*	100*	100*	100*	×	×	0	0	0	11
	+	×	×	×	×	×	0	0	0	0	×	×	×	×	×	10
	n389	×	×	×	×	×	100*	100*	100*	100*	×	×	×	×	×	10
	+	0	0	0	100	100	×	×	×	×	100	100	0	0	0	9
	n389	0	0	0	0	0	×	×	×	×	0	0	0	0	0	10
syIs49	+	100	0	0	0	100	100	0	0	100	100	0	0	0	100	107
	n389	0	0	0	0	0	0	0	0	0	0	0	0	0	0	104
	+	×	×	×	0	100	100	0	0	100	100	0	×	×	×	9
	n389	×	×	×	0	0	0	0	0	0	0	0	×	×	×	10
	+	100	0	0	×	×	100	0	0	100	×	×	0	0	100	9
	n389	0	0	0	×	×	0	0	0	0	×	×	0	0	0	10
	+	×	×	×	×	×	100	0	0	100	×	×	×	×	×	5
	n389	×	×	×	×	×	0	0	0	0	×	×	×	×	×	10
	+	100	0	0	0	100	×	×	×	×	100	0	0	0	100	5
	n389	0	0	0	0	0	×	×	×	×	0	0	0	0	0	10
syIs50	+	0	0	0	100	100	100	100	100	100	100	100	0	0	0	33
	n389	0	0	0	0	0	17†	71†	71†	17†	0	0	0	0	0	35
	+	×	×	×	100	100	100	100	100	100	100	100	×	×	×	7
	n389	×	×	×	0	0	25†	88†	88†	25†	0	0	×	×	×	8
	+	0	0	0	×	×	100	100	100	100	×	×	0	0	0	7
	n389	0	0	0	×	×	20†	81†	81†	20†	×	×	0	0	0	11
	+	×	×	×	×	×	100	100	100	100	×	×	×	×	×	11
	n389	×	×	×	×	×	25†	91†	75†	25†	×	×	×	×	×	12
	+	0	0	0	100	100	×	×	×	×	100	100	0	0	0	8
	n389	0	0	0	0	0	×	×	×	×	0	0	0	0	0	11
syIs54	+	0	100	100	100	0	0	0	0	0	0	100	100	100	0	77
	n389	0	0	0	0	0	0	0	0	0	0	0	0	0	0	83
	+	×	×	×	100	0	0	0	0	0	0	100	×	×	×	8
	n389	×	×	×	0	0	0	0	0	0	0	0	×	×	×	10
	+	0	100	100	×	×	0	0	0	0	×	×	90	90	0	8
	n389	0	0	0	×	×	0	0	0	0	×	×	0	0	0	10
	+	×	×	×	×	×	0	0	0	0	×	×	×	×	×	9
	n389	×	×	×	×	×	0	0	0	0	×	×	×	×	×	10
	+	0	100	100	100	0	×	×	×	×	0	100	100	100	0	10
	n389	0	0	0	0	0	×	×	×	×	0	0	0	0	0	10

Crosses (×) represent cell types whose precursors were ablated during Pn.px and Pn.pxx stages. Numbers are percentage of animals expressing *GFP* in the given cell type. A, B1, B2, C, D, E and F refer to differentiated vulval cell fates. Four different ablation sets were performed (A-B1-B2, C-D, A-B1-B2-C-D and E-F). The *GFP* integrants are *ayIs4 (egl-17::GFP)*, *syIs49 (zmp-1::GFP)*, *syIs50 (cdh-3::GFP)* and *syIs54 (ceh-2::GFP)*.

*Extremely weak GFP fluorescence.

†Weak GFP fluorescence compared with the wild-type *lin-11* genetic background.

Early expression of lin-11 in vulval cells determines the pattern of invagination

The vulval expression of *lin-11* suggests an earliest requirement in VPC daughters (Pn.px cells). In wild-type animals, the vulC and vulD cells of the 2° lineage invaginate during L4 stage (Fig. 1). A high level of *lin-11* expression in their precursors at Pn.px and Pn.pxx stages suggests that in wild-type animals, LIN-11 activity could specify the ability of cells to invaginate, consistent with the vulval invagination defect observed in *lin-11* mutant animals. To determine whether ectopic expression of *lin-11* can alter vulval cells fates and therefore invagination pattern, we generated transgenic animals carrying full-length *lin-11* genomic DNA under the control of the heat-shock promoter, *hsp16-41*. Such animals (*hs::lin-11*) were heat shocked at different stages (Pn.px, Pn.pxx and Pn.pxxx) and analyzed for the vulval morphology phenotype. Although the heat shock given at the Pn.pxxx stage did not cause a noticeable defect in vulval morphology, heat shocks at the other two stages caused ectopic invagination (Fig. 6). Specifically, the vulA, vulB1 and vulB2 cell types that normally remain adhered to the epidermis in wild type had invaginated (Fig. 6A,C; compare with wild-type in Fig. 7A). The defect was qualitatively similar after the heat shock at Pn.px or Pn.pxx stage, although the penetrance was higher at the Pn.px stage. In most cases, only a subset of the P5.p and P7.p lineage cells showed ectopic invagination (90%, *n*=19; Fig. 6A), although in one animal all vulval cells were completely invaginated (Fig. 6C). This phenotype suggests that ectopic expression of *lin-11* in the precursors of vulA, vulB1 and vulB2 interferes with their normal development, and possibly alters their cell fates. This hypothesis was further supported by our observation that in some cases (two out of

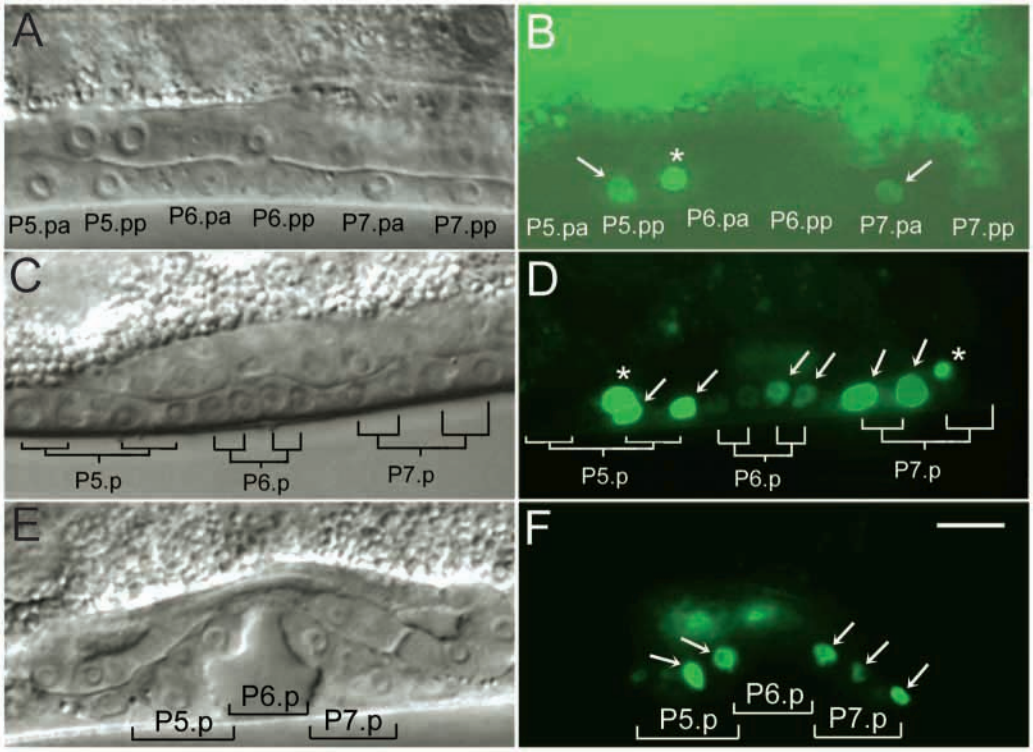

Fig. 4. Developmental expression of *lin-11::GFP (syIs80)* in vulval cells. (A,C,E) Nomarski photographs. (B,D,F) *lin-11::GFP*-expressing vulval cells marked with arrows. Few VC neurons are also visible (star). (A,B) During Pn.px stage, weak GFP fluorescence is detected in the P5.pp and P7.pa cells (arrows in B). (C,D) By Pn.pxx stage, vulval cells express high levels of *GFP*. The VPC lineage tree has been drawn. In this animal P5.ppx, P6.ppx and P7.pax cells are seen expressing *GFP*. (E,F) During L4 stage, Pn.pxxx cells express *GFP* in the P5.p and P7.p progeny. The region occupied by each VPC progeny has been marked. In this focal plane, only a subset of the cells is visible (arrows). Anterior is towards the left. Scale bar: 10 μm.

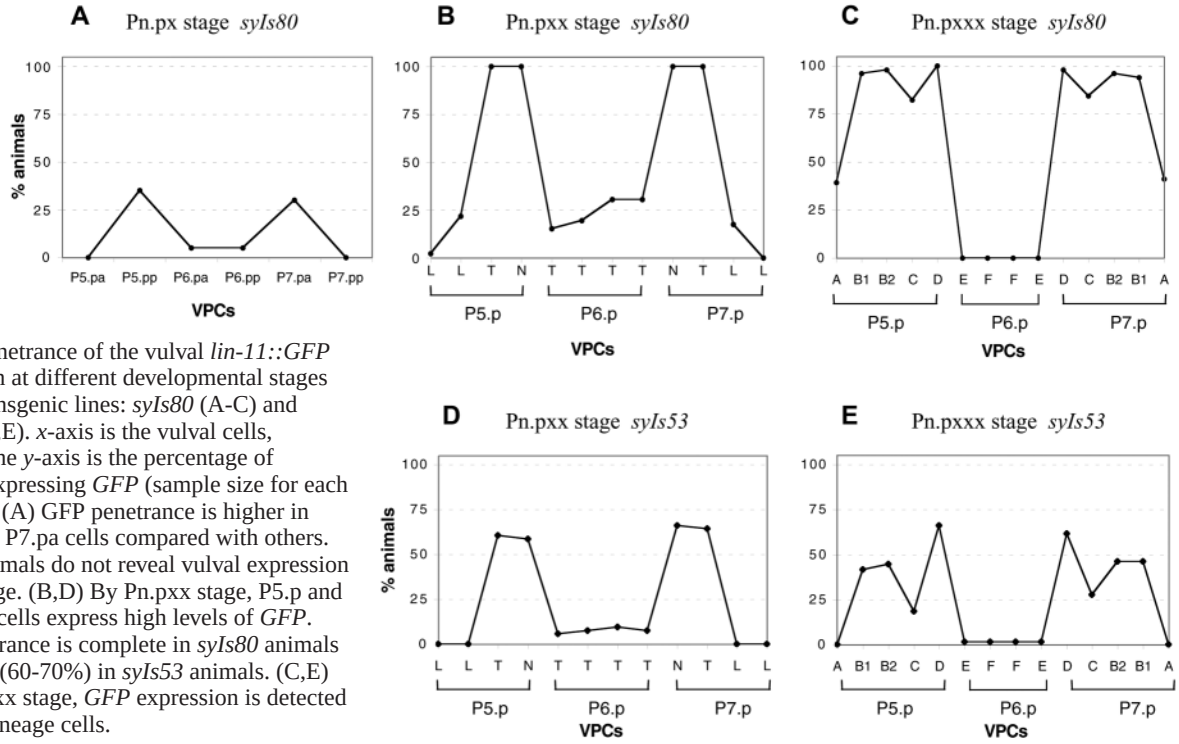

Fig. 5. Penetrance of the vulval *lin-11::GFP* expression at different developmental stages in two transgenic lines: *syIs80* (A-C) and *syIs53* (D,E). *x*-axis is the vulval cells, whereas the *y*-axis is the percentage of animals expressing *GFP* (sample size for each set is 50). (A) GFP penetrance is higher in P5.pp and P7.pa cells compared with others. *syIs53* animals do not reveal vulval expression at this stage. (B,D) By Pn.pxx stage, P5.p and P7.p N,T cells express high levels of *GFP*. The penetrance is complete in *syIs80* animals but lower (60-70%) in *syIs53* animals. (C,E) By Pn.pxxx stage, *GFP* expression is detected in all 2° lineage cells.

six) ectopically invaginated cells showed expression of the *egl-17::GFP*, a marker for wild-type vulC and vulD cell fates (see Fig. 6B for ectopic expression in P7.p lineage vulA; Fig. 3A,B shows wild-type pattern). By contrast, no such defect was observed in control heat shock experiment. We conclude that during Pn.px and Pn.pxx stages *lin-11* expression in the precursors of vulC and vulD promotes a wild-type vulval invagination.

In addition to the invagination defects, we observed a weak multivulva (Muv) phenotype from the heat shocks given during the early Pn.px stage (16%, *n*=69; average VPC induction 3.2). Two major signaling pathways that function during vulval

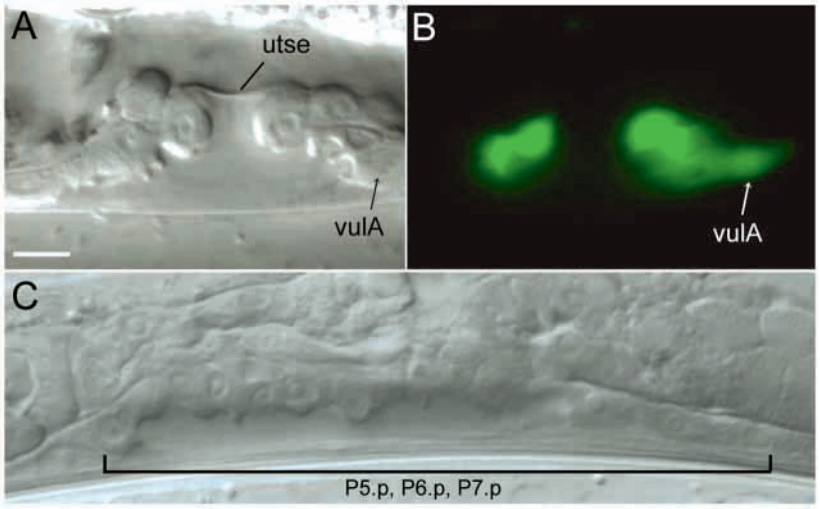

Fig. 6. Effect of the heat shock induced *lin-11* expression. (A) Pn.pxx stage heat pulse causes ectopic invagination in some of the P5.p and P7.p lineage cells. (B) The same animal as in A. The ectopic expression of *egl-17::GFP* can be seen in the presumptive vulA of the P7.p lineage. (C) In this animal (heat pulsed during Pn.px stage), all vulval cells have invaginated. The *hs::lin-11* transgenic strains are *syEx530* (A,B) and *syEx500* (C). utse, uterine seam cell. In all images, anterior is towards the left. Scale bar: 8 μm.

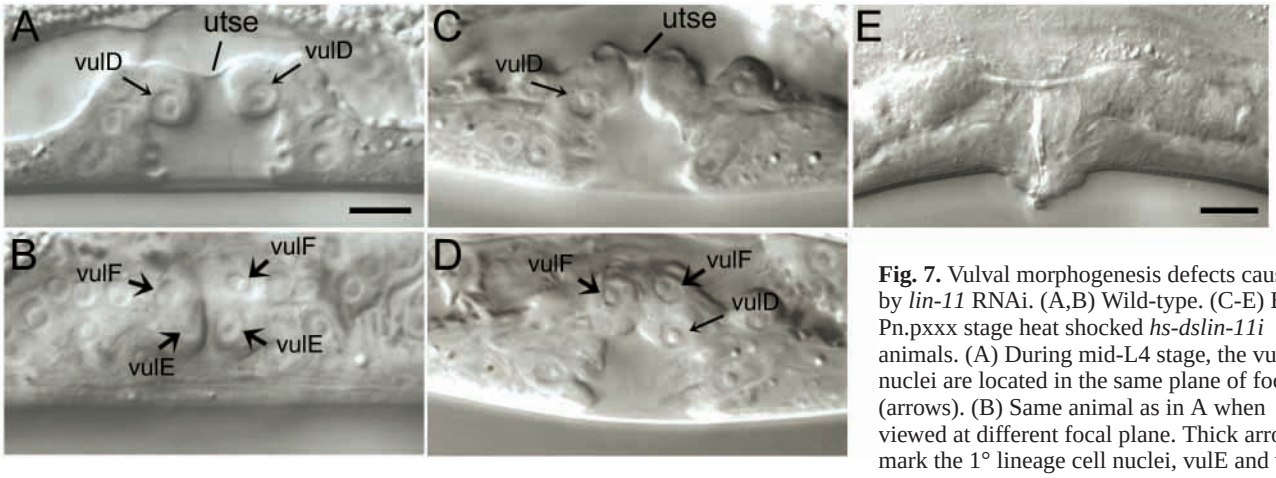

Fig. 7. Vulval morphogenesis defects caused by *lin-11* RNAi. (A,B) Wild-type. (C-E) Early Pn.pxxx stage heat shocked *hs-dslin-11i* animals. (A) During mid-L4 stage, the vulD nuclei are located in the same plane of focus (arrows). (B) Same animal as in A when viewed at different focal plane. Thick arrows mark the 1° lineage cell nuclei, vulE and vulF – all seen together. (C) A *hs-dslin-11i* animal having defects in the positioning of vulval nuclei. In this focal plane, only the P5.p lineage presumptive vulD nucleus is visible. (D) The same animal as in C when viewed at different focal plane. The presumptive vulD nucleus of the P7.p lineage (thin arrow) is seen along with the vulF nuclei (thick arrows). vulE pair is not visible in this plane. (E) A weak Pvul phenotype seen in some *hs-dslin-11i* adults. Anterior is towards the left. Scale bars: in A, 8 μm for A-D; in E, 10 μm.

induction are the EGF-receptor and LIN-12/Notch mediated pathways (reviewed by Greenwald, 1997; Wang and Sternberg, 2001). We tested the involvement of EGF-receptor signaling using a hypomorphic *lin-3* allele, *n378*, and observed complete suppression of the Muv phenotype. In addition, *hs::lin-11* does not suppress the vulval induction defect of *n378* (VPC induction 0.8, *n*=36 compared with the control *n378* heat-shocked animals 0.7, *n*=35). This epistasis of *n378* over *hs::lin-11* suggests that the effect of *lin-11* overexpression is likely to be upstream of *lin-3*, and possibly at the level of *lin-3* transcription. We are not convinced that such an effect of *lin-11* is physiologically relevant because none of the known alleles of *lin-11* exhibit defects in the extent of vulval induction, and *lin-11::GFP* transgenic animals (*nIs96*, *syIs80* and *syIs53*) do not reveal GFP fluorescence in the anchor cell (AC) during L2/L3 stages when AC is required for vulval induction. It is more likely that the overexpression of *lin-11* mimics the effect of some other homeodomain or LIM homeodomain protein.

lin-11 expression during terminal differentiation specifies vulval morphology

Our experiments so far have defined the function of *lin-11* during the Pn.px and Pn.pxx stages in establishing the correct pattern of vulval invagination. *lin-11* continues to be expressed at high levels in Pn.pxxx cells and thus might be required for vulval differentiation. To test this hypothesis, we used a conditional RNAi approach to inactivate *lin-11* gene function. We generated transgenic *hs-dslin-11i* animals (carrying *lin-11* cDNA in sense and antisense orientations under control of the *hsp16-41* heat-shock promoter) that can be heat shocked at any desired developmental stage to induce the formation of double-stranded RNA. As a control, we heat shocked *hs-dslin-11i* animals during early L3 stage (Pn.p cells in Fig. 1) and compared the vulval morphology and egg-laying phenotypes with the *lin-11* loss of function alleles. Forty percent (*n*=8) of the heat-shocked animals showed an egg-laying defective (Egl) phenotype and a weak vulval invagination defect similar to the *lin-11(n566)* allele. One of them also exhibited the AC

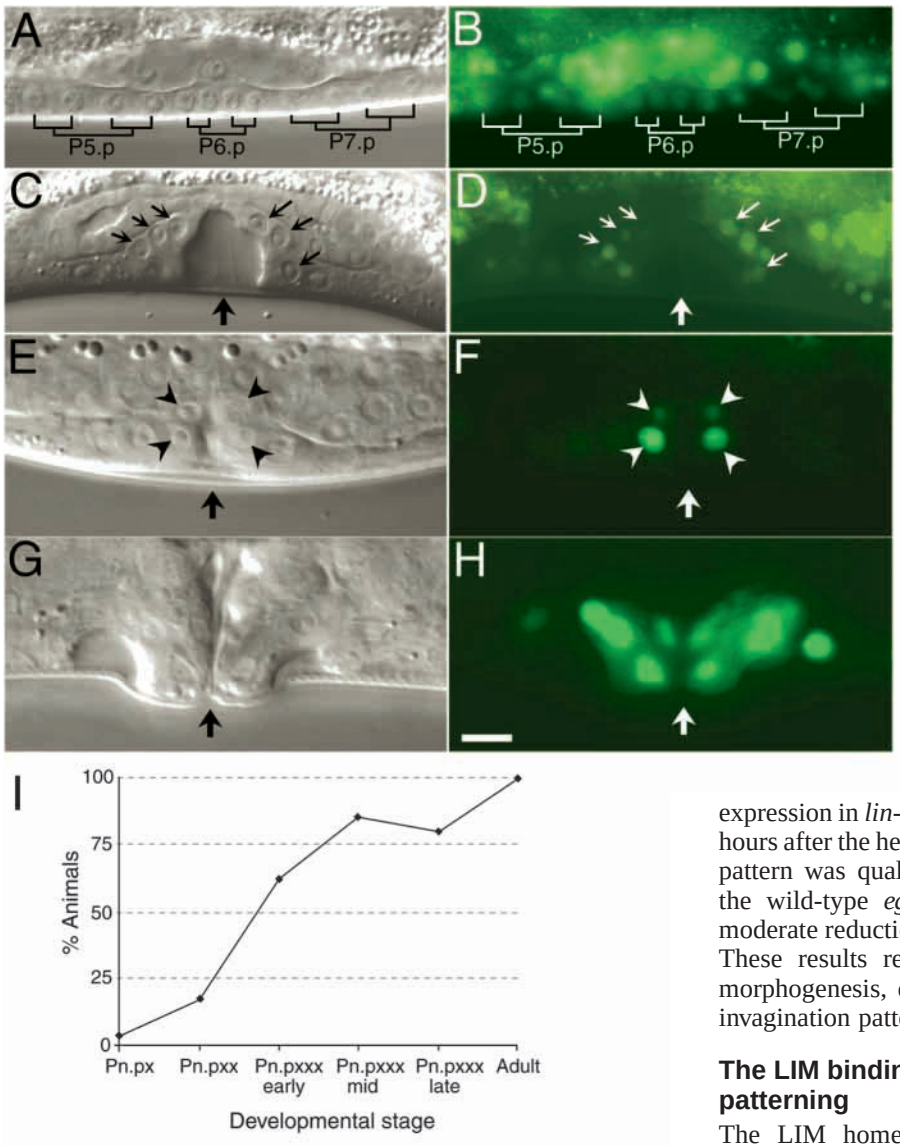

Fig. 8. Expression pattern of *ldb-1* during vulval development. Thick arrows indicate vulval opening. (A,C,E,G) Nomarski images, (B,D,F,H) GFP fluorescence photomicrographs. Number of animals examined at each stage are 28 (Pn.px), 25 (Pn.pxx), 34 (early Pn.pxxx), 26 (mid Pn.pxxx), 15 (late Pn.pxxx) and 13 (adult). (A,B) Pn.pxx stage animal expressing faint *ldb-1::GFP* in vulval progeny. Vulval lineages are drawn. (C,D) An early-L4 stage animal, arrows indicate some of the cells expressing *GFP*. (E,F) A mid-L4 stage animal. Arrowheads indicate all 1° lineage cells in this focal plane that are expressing *GFP*. (G,H) A young adult expressing *GFP* in all the 2° lineage cells. (I) Penetrance of *ldb-1::GFP* expression at different stages. Anterior is towards the left. Scale bar: 10 μm.

migration defect, a phenotype that contributes to the Egl defect in *lin-11* mutant animals (Newman et al., 1999). In control heat-shocked animals (no *hs-dslin-11i*), no such defect was observed (n=20). These results confirm that the RNAi phenotypes of *hs-dslin-11i* animals are due to the reduction in the wild-type *lin-11* gene function. Next, we examined the effect of the *lin-11* RNAi on vulval morphology by heat shocking *hs-dslin-11i* animals during early Pn.pxxx stage (early-L4). In wild-type animals during the mid-L4 stage, vulval nuclei occupy stereotypical positions, such that vulD nuclei of the P5.p and P7.p lineage are located in the same plane of focus (Fig. 7A). Likewise, vulE and vulF nuclei are seen in one focal plane, different from that occupied by vulD nuclei (Fig. 7B). By contrast, the heat-shocked *hs-dslin-11i* animals showed significant defects in the vulval morphology with misplaced vulval nuclei (30%, n=16; Fig. 7C,D). Specifically, we found that vulC and vulD nuclei were located in wrong focal planes (vulD is shown in Fig. 7C,D). Two out of five defective animals also showed abnormal positioning of the nuclei of 1° lineage cells (see Fig. 7D for vulF position, vulE nuclei are not seen in this plane). Overall, vulval invagination was narrower along the anteroposterior axis compared with the wild type. This abnormal morphology was correlated with a protruding vulva phenotype at the adult stage (Fig. 7E). However, such animals were able to lay eggs normally.

We also examined *egl-17::GFP* expression in *lin-11* RNAi animals during the mid-L4 stage (~4 hours after the heat shock treatment). Although the overall GFP pattern was qualitatively wild type (n=9; see Fig. 3A,B for the wild-type *egl-17::GFP* pattern), two worms did show moderate reduction in the GFP fluorescence in vulC and vulD. These results reveal a novel function of *lin-11* in vulval morphogenesis, distinct from its early role in specifying the invagination pattern.

The LIM binding protein LDB-1 plays a role in vulval patterning

The LIM homeodomain proteins contain a pair of LIM domains that interact with co-factors and modulate protein activity (Dawid et al., 1998; Bach, 2000; Hobert and Westphal, 2000). Among the co-factors are the LIM-binding proteins represented by NLI/Ldb1/CLIM2, which display highly specific interactions with the LIM domains. The *C. elegans* LIM-binding protein LDB-1 has been shown to interact with two LIM homeodomain proteins CEH-14 and MEC-3 (Cassata et al., 2000). As it is the only known LIM-binding protein in *C. elegans*, it is likely that LDB-1 regulates the activities of other LIM homeodomain proteins, including LIN-11.

To investigate the role of *ldb-1* during vulval development, we examined its expression using a *ldb-1::GFP* construct. *ldb-1::GFP* expression is first detected in embryos towards the end of gastrulation (prior to the comma stage) and is seen in the vulval cells among other expression (Cassata et al., 2000) (not shown). In vulval cells *ldb-1::GFP* expression is observed in both the 1° as well as 2° lineage cells (Fig. 8). Expression during the Pn.px stage was rarely observed (<5%, n=28; Fig. 8I). During Pn.pxx stage, a weak and low penetrant *GFP* could be detected in 1° and 2° lineage cells (16%, n=25; Fig. 8A,B,I). However, by the Pn.pxxx stage strong and highly penetrant *ldb-1::GFP* expression could be detected in all vulval progeny

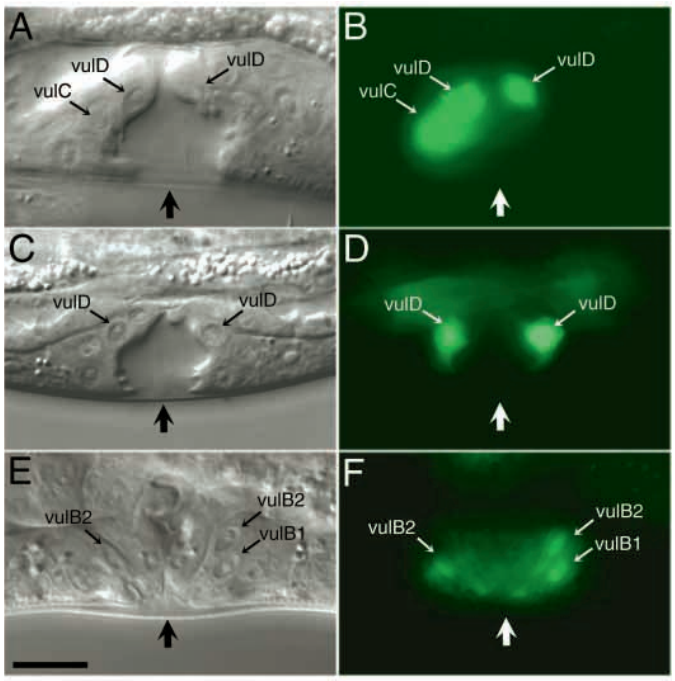

Fig. 9. Effect of *ldb-1* RNAi on vulval morphology and marker gene expression. Vulval cells are marked with thin arrows. Thick arrows indicate the position of the vulval opening. Nomarski images showing morphological defects in the vulva during mid (A,C) and late (E) L4 stages. (B,D,F) GFP fluorescence photomicrographs of the corresponding animals. (A,B) P7.p lineage presumptive vulC fails to express *egl-17::GFP (ayIs4)*. (C,D) Only presumptive vulD, but not presumptive vulC, vulE and vulF, are expressing *cdh-3::GFP (syIs50)*. (E,F) Presumptive vulC of P5.p and P7.p lineage, and presumptive vulB1 of the P5.p lineage fail to express *ceh-2::GFP (syIs54)*. Anterior is towards the left. Scale bar: 10 μm.

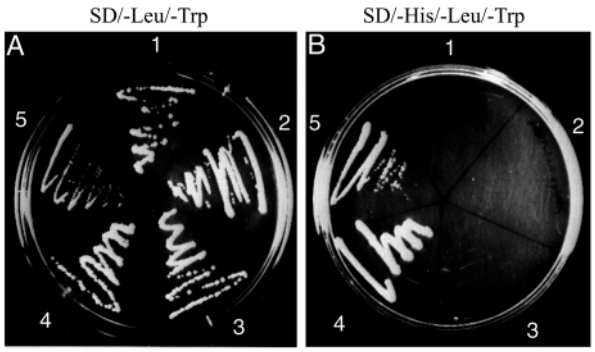

Fig. 10. Yeast two-hybrid interaction test of LIN-11 and LDB-1. Yeast cells were transformed with plasmids pGBKT7 and pGADT7 (1), pGBKT7-lin-11 and pGADT7 (2), pGBKT7 and pGADT7-ldb-1 (3), pVA3 and pTD1 (4), and pGBKT7-lin-11 and pGADT7-ldb-1 (5). In a transformation control (A), all cells can be seen growing on plate that lacks leucine and tryptophan (SD/–Leu/–Trp). However, only positive control (pVA3 and pTD1) and test (pGBKT7-lin-11 and pGADT7-ldb-1) can promote *HIS3* expression (B), leading to growth on plate that lacks histidine, leucine and tryptophan (SD/–His/–Leu/–Trp).

(Fig. 8C-F,I). Expression was also observed during early adult stage (Fig. 8G-I).

We examined the effect of decreasing *ldb-1* activity using RNAi. *ldb-1* RNAi animals showed uncoordinated movement and failed to respond to touch, a phenotype that has been previously described (Cassatta et al., 2000) (not shown). We also observed defects in vulval morphology and gonad arms at significant frequencies (vulval defect: 26%, *n*=101, see Fig. 9; gonad defect: 40%, *n*=18). Vulval phenotypes included abnormal placement of the 1° and 2° lineage cells (Fig. 9A,C,E). Occasionally, animals displayed a protruding vulva phenotype and were Egl. We did not observe a vulval invagination defect in any of the RNAi animals. We also examined the effect of *ldb-1* RNAi on vulval markers, *egl-17::GFP*, *zmp-1::GFP*, *cdh-3::GFP* and *ceh-2::GFP*. In all but the case of *zmp-1::GFP*, GFP fluorescence was altered (Fig. 9, compare with wild-type patterns in Fig. 3). *egl-17::GFP* expression was frequently absent in the presumptive vulC (Fig. 9A,B). The *cdh-3::GFP* showed reduced or no expression (Fig. 9C,D shows only vulD expression). *ceh-2::GFP* expression in the presumptive vulB1/B2 cells was variable and weak, whereas presumptive vulC often showed no expression (Fig. 9E,F). In control RNAi animals, no such defects were observed. Thus, LDB-1 plays a role in vulval morphogenesis. In *Drosophila*, the LIM homeodomain protein Apterous and its LIM-binding partner Chip form a regulatory feedback network to modulate the expression of each other (Milan and Cohen, 2000). We examined the possibility of such feedback regulation between LDB-1 and LIN-11, but found no change in the expression of *lin-11::GFP* in *ldb-1* RNAi animals.

LDB-1 and LIN-11 interact in yeast two-hybrid assay

We examined physical interaction between LIN-11 and LDB-1 using a two-hybrid interaction assay (Fields and Song, 1989). For this, we designed two separate expression constructs. One construct expresses LIM domains of LIN-11 as a fusion protein with the GAL4 DNA-binding domain, whereas the other expresses LDB-1 LIM-interacting domain (LID) fused to the GAL4 activation domain (see Materials and Methods). Fig. 10B shows that fusion proteins involving LIN-11 LIM domains and LDB-1 LID interact with each other thereby leading to the growth of yeast cells on plates lacking histidine, leucine and tryptophan. Neither one alone (Fig. 10B-2,B-3) is sufficient for *HIS3* expression. In a control experiment (Fig. 10A), all transformants grew on plates lacking leucine and tryptophan. These results demonstrate a physical interaction between LIN-11 and LDB-1.

DISCUSSION

lin-11 is necessary for the development of all vulval cell types

Earlier studies on *lin-11* using cell lineage (Ferguson et al., 1987) and *lin-11::lacZ* expression (G. A. Freyd, PhD thesis, Massachusetts Institute of Technology, 1991) (Struhl et al., 1993) have shown its function in specifying the vulC and vulD cell types. Our results extend these findings and demonstrate that *lin-11* is necessary for the differentiation of all vulval cell types, including the 1° lineage cells.

In wild-type *C. elegans* during the L4 stage, vulval cells

initiate the process of invagination (Fig. 1) and specific cell fusion to give rise to the adult structure. The cell fusion events are ordered and occur only between the homologous cell types, e.g. P5.p lineage vulA fuses only with the P7.p lineage vulA (Sharma-Kishore et al., 1999). By contrast, *lin-11* mutant vulval cells exhibit defects in cell fusion events. Often all 2° lineage vulval cells fuse together, suggesting that they have acquired a common fate. However, this fate is distinct from any of the wild-type cell fates as none of the examined markers (*egl-17::GFP, zmp-1::GFP, cdh-3::GFP* and *ceh-2::GFP*) is expressed in *lin-11* mutant vulval cells. Using cell ablation experiments, we have shown that defects in cell fusion events and marker gene expression in *lin-11* mutant animals result from cell-autonomous requirements of *lin-11*. The phenomenon of a cell fusion defect is similar to that observed for ray fusion in *C. elegans* mutants affecting male tail development (Baird et al., 1991; Chow and Emmons, 1994).

Analysis of the *ajm-1::GFP* expression in 1° vulval cells in *lin-11* animals has revealed defects in the morphology of vulE and vulF rings, consistent with the abnormal patterns of *egl-17::GFP, cdh-3::GFP* and *zmp-1::GFP* expression (see Fig. 3). Hence, the 1° lineage cells are not likely to form a functional vulval opening. These results are consistent with our previous findings on tissue-specific regulation of *lin-11*, where we used vulval- and uterine-specific regulatory elements of *lin-11* to demonstrate that wild-type egg-laying requires *lin-11* function in both the vulva and the uterine π lineage cells (Gupta and Sternberg, 2002).

The vulval cell fusion defects in *lin-11* mutant animals could arise because *lin-11* directly regulates the process of cell fusion or as a consequence of abnormal differentiation. Two sets of results support the latter possibility. First, *lin-11* expression in vulval cells is detected beginning at the Pn.px stage (see Fig. 4). Second, induction of *lin-11* RNAi (using *hs-dslin-11i*) during mid-L4 stage causes no significant effect on the formation of vulval rings. Thus, during terminal differentiation, *lin-11* mutant vulval cells might fail to express cell-type specific genes, leading to the defects in fate specification. The abnormal cell fusion is the consequence of cells failing to acquire their unique identities. Such a role of *lin-11* in the vulva is similar to that of *C. elegans* LIM homeobox gene, *mec-3*, in touch receptor neurons. In *mec-3* mutant animals, the presumptive touch neurons are generated but fail to acquire the correct identity (Way and Chalfie, 1988).

Temporal expression of *lin-11* promotes distinct vulval cell fates

LIM homeobox genes have been shown to express in highly restricted spatial and temporal manner (Bach, 2000; Hobert and Westphal, 2000). Wing development in *Drosophila* requires dynamic expression of the LIM homeobox gene *apterous*. The level and domain of *apterous* expression are highly regulated and help define the dorsoventral boundary leading to wing growth and patterning (Diaz-Benjumea and Cohen, 1993; Milan and Cohen, 2000).

The dynamic expression of *lin-11* in vulval cells can be classified into two distinct patterns: an initial polarized expression (during Pn.px and Pn.pxx stages) where only a subset of the cells express *lin-11*, and a broad pattern of expression during terminal differentiation (Pn.pxxx cells) where all 2° lineage cells express *lin-11*. We hypothesized that these two different patterns of *lin-11* expression may have different functions and tested the hypothesis experimentally. First, a *hs::lin-11* system was used to express *lin-11* ectopically in all vulval cells during Pn.px and Pn.pxx stages. This led to defects in vulval invagination caused by the failure of presumptive vulA, vulB1 and vulB2 to remain adhered to the epidermis (Fig. 6; wild-type pattern in Fig. 1). Second, using a RNAi approach, we inhibited *lin-11* function during early Pn.pxxx stage when *lin-11* is expressed in all 2° lineage cells. The *lin-11* RNAi animals showed defects in vulval morphology and vulval nuclei failed to occupy stereotypic positions. This phenotype is likely to result from a differentiation defect in vulval progeny.

The two distinct requirements of *lin-11* in vulval cells are likely to be mediated by different target genes. The vulval invagination defect in *lin-11* animals suggests that one potential target of *lin-11* could be the genes that regulate epithelial morphogenesis. Our reporter gene expression studies have identified a cadherin family member, *cdh-3*, that functions downstream of *lin-11*. In *lin-11* mutant vulval cells *cdh-3::GFP* expression in the presumptive vulC and vulD is abolished (Fig. 3; Table 1). Cadherins are known to regulate epithelial morphogenesis by mediating adhesions between cell-cell and cell-extracellular matrix (Gumbiner, 1996). However, the function of *cdh-3* in vulval development is not essential, perhaps owing to redundancy.

The early expression of *lin-11* is polarized and confers identity on cells to give rise to progeny (vulC and vulD) that invaginate during L4 stage (see Fig. 1). This conclusion is also supported by the roles of *lin-17* (a *frizzled* family member) (Sawa et al., 1996) and *lin-11* during vulval development (Gupta and Sternberg, 2002). In *lin-17* mutant animals, *lin-11* expression in P7.p lineage cells is often reversed, i.e. LL lineage cells begin to express *lin-11* instead of the wild-type NT lineage cells. This reversal in the polarity of *lin-11* expression correlates with the opposite orientation of invagination of the P7.p lineage cells. A similar role for *lin-11* has also been demonstrated in the specification of the ASG and AWA neurons (Sarafi-Reinach et al., 2001). Although during embryonic stages both neurons express *lin-11*, expression in AWA is lost by the L1 larval stage and persists only in the ASG neuron. This later stage expression of *lin-11* in ASG is necessary for its wild-type development. If *lin-11* is ectopically expressed in AWA during post-L1 larval stages, the AWA adopts partial ASG-like features. Similar functions of other LIM homeobox genes in determining polarity or asymmetric cell fates have also been demonstrated. *C. elegans lim-6*, another LIM homeobox gene, generates functional differences in the chemosensory behavior between a pair of neurons ASEL/R (Pierce-Shimomura et al., 2001). In mouse embryonic axis formation, the role of *lim1* in anterior-posterior polarity is also suggestive of such a biological function (Perea-Gomez et al., 1999). In this case, *lim1* expression in the anterior region cells of the visceral endoderm confers anterior identity and makes them different from the posterior cells. Thus, the role of the LIM homeobox genes in generating cellular asymmetry appears to be a conserved biological function.

Functional specificity of LIN-11 during vulval development

How does *lin-11* play different roles at different stages of

vulval development? One possibility could be that LIN-11 interacts with stage- and cell-type specific factors to bring about the different outcomes. The LIM domains of the LIM homeodomain proteins are known to serve as protein-protein interacting interface that promote the formation of multimeric complexes and influence DNA-binding affinity of the homeodomain (Dawid et al., 1998). Many studies have revealed the presence of LIM domain-binding proteins (Dawid et al., 1998; Bach, 2000; Hobert and Westphal, 2000). Although a majority of them belong to the NLI/Ldb1/CLIM2 family, others such as POU homeodomain factor Pit1 (Bach et al., 1995), WD40 repeat containing factor SLB (Howard and Maurer, 2000) and bHLH factor E47 (German et al., 1992) have also been identified.

The *C. elegans* LIM-binding protein LDB-1 was previously shown to be required for the wild-type functioning of several neurons (Cassata et al., 2000). We find that *ldb-1* is expressed in both the 1° as well as 2° lineage vulval cells, a pattern that overlaps with *lin-11* expression. Analysis of the *ldb-1* vulval expression has revealed some differences from *lin-11*. During Pn.pxx stage, *lin-11::GFP* shows alternating low and high pattern of expression in P5.p and P7.p lineage cells (LLHH-HHLL, respectively, from anterior to posterior; L, low; H, high). *ldb-1::GFP*, however, shows no such pattern and is detected at uniform level in all 1° and 2° lineage cells. In addition, *ldb-1::GFP* continues to be expressed at high levels in 1° vulval progeny during L4 and young adult stages, whereas *lin-11::GFP* expression in 1° lineage cells is significantly weaker compared with the 2° lineage cells. Hence, LDB-1 may regulate only a subset of the LIN-11 functions. Consistent with this, *ldb-1* RNAi animals did not show defects in vulval invagination but in vulval morphology (Figs 7, 9). However, it is possible that *ldb-1* RNAi effect is weak because of the partial elimination of gene activity. Our findings that LIN-11 and LDB-1 physically interact support the hypothesis that LIN-11 and LDB-1 function together to regulate vulval differentiation. Furthermore, these results suggest that *lin-11* may use other mechanisms during earlier stages of vulval development.

We thank S. Cameron, D. Sherwood and T. Inoue for integrated strains. Robert Oania provided assistance in two-hybrid experiments. Some of the strains were obtained from *Caenorhabditis* Genetics Center. We also thank D. Sherwood, T. Inoue and anonymous reviewers for comments on the manuscript. This work was supported by funds from the HHMI and USPHS grant HD23690 to P.W.S. B.P.G. was supported by a long-term fellowship from HFSP and as an associate of the HHMI. M.W. was an AMGEN fellow. P.W.S. is an investigator of the HHMI.

REFERENCES

Ambros, V. (1999). Cell cycle-dependent sequencing of cell fate decisions in *Caenorhabditis elegans* vulva precursor cells. *Development* **126**, 1947-1956.

Avery, L. and Horvitz, H. R. (1987). A cell that dies during wild-type *C. elegans* development can function as a neuron in a *ced-3* mutant. *Cell* **51**, 1071-1078.

Bach, I., Rhodes, S. J., Pearse, R. V., II, Heinzel, T., Gloss, B., Scully, K. M., Sawchenko, P. E. and Rosenfeld, M. G. (1995). P-Lim, a LIM homeodomain factor, is expressed during pituitary organ and cell commitment and synergizes with Pit-1. *Proc. Natl. Acad. Sci. USA* **92**, 2720-2724.

Bach, I. (2000). The LIM domain: regulation by association. *Mech. Dev.* **91**, 5-17.

Baird, S. E., Fitch, D. H. A., Kassem, I. A. A. and Emmons, S. W. (1991). Pattern formation in the nematode epidermis: determination of the arrangement of peripheral sense organs in the *C. elegans* male tail. *Development* **113**, 515-526.

Brenner, S. (1974). The genetics of *Caenorhabditis elegans*. *Genetics* **77**, 71-94.

Burdine, R. D., Branda, C. S. and Stern, M. J. (1998). EGL-17(FGF) expression coordinates the attraction of the migrating sex myoblasts with vulval induction in *C. elegans*. *Development* **125**, 1083-1093.

Cassata, G., Röhrig, S., Kuhn, F., Hauri, H.-P., Baumeister, R. and Bürglin, T. R. (2000). The *Caenorhabditis elegans* Ldb/NLI/Clim orthologue *ldb-1* is required for neuronal function. *Dev. Biol.* **226**, 45-56.

Chow, K. L. and Emmons, S. W. (1994). HOM-C/HOX genes and four interacting loci determine the morphogenetic properties of single cells in the nematode male tail. *Development* **120**, 2579-2593.

Cohen, B., McGuffin, M. E., Pfeifle, C., Segal, D. and Cohen, S. (1992). *apterous*, a gene required for imaginal disc development in *Drosophila* encodes a member of the LIM family of developmental regulatory proteins. *Genes Dev.* **6**, 715-729.

Costa, M., Raich, W., Agbunag, C., Leung, B., Hardin, J. and Priess, J. R. (1998). A putative catenin-cadherin system mediates morphogenesis of the *Caenorhabditis elegans* embryo. *J. Cell Biol.* **141**, 297-308.

Dawid, I. B., Breen, J. J. and Toyama, R. (1998). LIM domains: multiple roles as adaptors and functional modifiers in protein interactions. *Trends Genet* **14**, 156-162.

Diaz-Benjumea, F. J. and Cohen, S. M. (1993). Interaction between dorsal and ventral cells in the imaginal discs directs wing development in *Drosophila*. *Cell* **75**, 741-752.

Dreyer, S. D., Zhou, G., Baldini, A., Winterpacht, A., Zabel, B., Cole, W., Johnson, R. L. and Lee, B. (1998). Mutations in *LMX1B* cause abnormal skeletal patterning and renal dysplasia in nail patella syndrome. *Nat. Genet.* **19**, 47-50.

Ferguson, E. L. and Horvitz, H. R. (1985). Identification and characterization of 22 genes that affect the vulval cell lineages of the nematode *Caenorhabditis elegans*. *Genetics* **110**, 17-72.

Ferguson, E. L., Sternberg, P. W. and Horvitz, H. R. (1987). A genetic pathway for the specification of the vulval cell lineages of *Caenorhabditis elegans*. *Nature* **326**, 259-267.

Fields, S. and Song, O.-K. (1989). A novel genetic system to detect protein-protein interactions. *Nature* **340**, 245-246.

Freyd, G., Kim, S. K. and Horvitz, H. R. (1990). Novel cystein-rich motif and homeodomain in the product of the *Caenorhabditis elegans* cell lineage gene *lin-11*. *Nature* **344**, 876-879.

German, M. S., Wang, J., Chadwick, R. B. and Rutter, W. J. (1992). Synergistic activation of the insulin gene by a LIM-homeodomain protein and a basic helix-loop-helix protein, building a functional insulin minienhancer complex. *Genes Dev.* **6**, 2165-2176.

Greenwald, I. (1997). Development of the vulva. In C. elegans *II* (ed. D. Riddle, T. Blumenthal, B. Meyer and J. Priess), pp. 519-541. Cold Spring Harbor, New York: Cold Spring Harbor Laboratory Press.

Gumbiner, B. M. (1996). Cell adhesion: the molecular basis of tissue architecture and morphogenesis. *Cell* **84**, 345-357.

Gupta, B. P. and Sternberg, P. W. (2002). Tissue-specific regulation of the LIM homeobox gene *lin-11* during development of the *Caenorhabditis elegans* egg-laying system. *Dev. Biol.* **247**, 102-115.

Hill, E., Broadbent, I. D., Chothia, C. and Pettitt, J. (2001). Cadherin superfamily proteins in *Caenorhabditis elegans* and *Drosophila melanogaster*. *J. Mol. Biol.* **305**, 1011-1024.

Hobert, O. and Westphal, H. (2000). Functions of LIM-homeobox genes. *Trends Genet.* **16**, 75-83.

Hobert, O., DíAlberti, T., Liu, Y. and Ruvkun, G. (1998). Control of neural development and function in a thermoregulatory network by the LIM homeobox gene *lin-11*. *J. Neurosci.* **18**, 2084-2096.

Howard, P. W. and Maurer, R. A. (2000). Identification of a conserved protein that interacts with specific LIM homeodomain transcription factors. *J. Biol. Chem.* **275**, 13336-13342.

Inoue, T., Sherwood, D. R., Aspock, G., Butler, J. A., Gupta, B. P., Kirouac, M., Wang, M., Lee, P. Y., Kramer, J. M., Hope, I. et al. (2002). Gene expression markers for *C. elegans* vulval cells. *Mech. Dev. Gene Exp. Patt.* **2**, 235-241.

Karlsson, O., Thor, S., Norberg, T., Ohlsson, H. and Edlund, T. (1990). Insulin gene enhancer binding protein Isl-1 is a member of a novel class of proteins containing both a homeo- and a Cys-His domain. *Nature* **344**, 879-882.

Mello, C. and Fire, A. (1995). DNA transformation. In Caenorhabditis elegans, *Modern biological analysis of an organism* (*Methods in Cell Biology*). Vol. 48 (ed. H. F. Epstein and D. C. Shakes), pp. 451-482. New York: Academic Press.

Mello, C. C., Kramer, J. M., Stinchcomb, D. and Ambros, V. (1991). Efficient gene transfer in *C. elegans* after microinjection of DNA into germline cytoplasm: Recombination drives the assembly of heritable transgenic structures. *EMBO J.* **10**, 3959-3970.

Milan, M. and Cohen, S. M. (2000). Temporal regulation of Apterous activity during development of the *Drosophila* wing. *Development* **127**, 3069-3078.

Mohler, W. A., Simske, J. S., Williams-Masson, E. M., Hardin, J. D. and White, J. G. (1998). Dynamics and ultrastructure of developmental cell fusions in the *Caenorhabditis elegans* hypodermis. *Curr. Biol.* **8**, 1087-1090.

Newman, A. P., Acton, G. Z., Hartwieg, E., Horvitz, H. R. and Sternberg, P. W. (1999). The *lin-11* LIM domain transcription factor is necessary for morphogenesis of *C. elegans* uterine cells. *Development* **126**, 5319-5326.

Perea-Gomez, A., Shawlot, W., Sasaki, H., Behringer, R. R. and Ang, S.-L. (1999). HNF3b and Lim1 interact in the visceral endoderm to regulate primitive streak formation and anterior-posterior polarity in the mouse embryo. *Development* **126**, 4499-4511.

Pettitt, J., Wood, W. B. and Plasterk, R. H. A. (1996). *cdh-3*, a gene encoding a member of the cadherin superfamily, functions in epithelial cell morphogenesis in *Caenorhabditis elegans*. *Development* **122**, 4149-4157.

Pfaff, S. L., Mendelsohn, M., Stewart, C. L., Edlund, T. and Jessell, T. M. (1996). Requirement for LIM homeobox gene Isl1 in motor neuron generation reveals a motor neuron-dependent step in interneuron differentiation. *Cell* **84**, 309-320.

Pierce-Shimomura, J. T., Faumont, S., Gaston, M. R., Pearson, B. J. and Lockery, S. R. (2001). The homeobox gene *lim6* is required for distinct chemosensory representations in *C. elegans*. *Nature* **410**, 694-698.

Podbilewicz, B. and White, J. G. (1994). Cell fusions in the developing epithelia of *C. elegans*. *Dev. Biol.* **161**, 408-424.

Porter, F. D., Drago, J., Xu, Y., Cheema, S. S., Wassif, C., Huang, S. P., Lee, E., Grinberg, A., Massalas, J. S., Bodine, D. et al. (1997). Lhx2, a LIM homeodomain gene, is required for eye, forebrain, and definitive erythrocyte development. *Development* **124**, 2935-2944.

Raich, W. B., Agbunag, C. and Hardin, J. (1999). Rapid epithelial-sheet sealing in the *Caenorhabditis elegans* embryo requires cadherin-dependent filopodial priming. *Curr. Biol.* **9**, 1139-1146.

Reddien, P. W., Cameron, S. and Horvitz, H. R. (2001). Phagocytosis promotes programmed cell death in *C. elegans*. *Nature* **412**, 198-202.

Rodriguez-Esteban, C., Schwabe, J. W., Pena, J. D., Rincon-Limas, D. E., Magallon, J., Botas, J., Izpisúa Belmonte, J. C. (1998). Lhx2, a vertebrate homologue of apterous, regulates vertebrate limb outgrowth. *Development* **125**, 3925-3934.

Ruvkun, G. and Hobert, O. (1998). The taxonomy of developmental control in *Caenorhabditis elegans*. *Science* **282**, 2033-2041.

Sarafi-Reinach, T. R., Melkman, T., Hobert, O. and Sengupta, P. (2001). The *lin-11* LIM homeobox gene specifies olfactory and chemosensory neuron fates in *C. elegans*. *Development* **128**, 3269-3281.

Sawa, H., Lobel, L. and Horvitz, H. R. (1996). The *Caenorhabditis elegans* gene *lin-17*, which is required for certain asymmetric cell divisions, encodes a putative seven-transmembrane protein similar to the *Drosophila* Frizzled protein. *Genes Dev.* **10**, 2189-2197.

Sharma-Kishore, R., White, J. G., Southgate, E. and Podbilewicz, B. (1999). Formation of the vulva in *Caenorhabditis elegans*: a paradigm for organogenesis. *Development* **126**, 691-699.

Struhl, G., Fitzgerald, K. and Greenwald, I. (1993). Intrinsic activity of the Lin-12 and Notch intracellular domains in vivo. *Cell* **74**, 331-345.

Sulston, J. E. and Horvitz, H. R. (1977). Post-embryonic cell lineages of the nematode, *Caenorhabditis elegans*. *Dev. Biol.* **56**, 110-156.

Tabara, H., Grishok, A. and Mello, C. C. (1998). RNAi in *C. elegans*: soaking in the genome sequence. *Science* **282**, 430-431.

Takuma, N., Sheng, H. Z., Furuta, Y., Ward, J. M., Sharma, K., Hogan, B. L., Pfaff, S. L., Westphal, H., Kimura, S. and Mahon, K. A. (1998). Formation of Rathke's pouch requires dual induction from the diencephalon. *Development* **125**, 4835-4840.

Vollrath, D., Jaramillo-Babb, V. L., Clough, M. V., McIntosh, I., Scott, K. M., Lichter, P. R. and Richards, J. E. (1998). Loss-of-function mutations in the LIM-homeodomain gene, *LMB1B*, in nail-patella syndrome. *Hum. Mol. Genet.* **7**, 1091-1098.

Wang, M. and Sternberg, P. W. (1999). Competence and commitment of *Caenorhabditis elegans* vulval precursor cells. *Dev. Biol.* **212**, 12-24.

Wang, M. and Sternberg, P. W. (2000). Patterning of the *C. elegans* 1° vulval lineage by RAS and Wnt pathways. *Development* **127**, 5047-5058.

Wang, M. and Sternberg, P. W. (2001). Pattern formation during *C. elegans* vulval induction. *Curr. Top. Dev. Biol.* **51**, 189-220.

Way, J. C. and Chalfie, M. (1988). *mec-3*, a homeobox-containing gene that specifies differentiation of the touch receptor neurons in *C. elegans*. *Cell* **54**, 5-16.

Way, J. C., Wang, L., Run, J.-Q. and Wang, A. (1991). The *mec-3* gene contains cis-acting elements mediating positive and negative regulation in cells produced by asymmetric cell division in *Caenorhabditis elegans*. *Genes Dev.* **5**, 2199-2211.

Wood, W. B. (1988). *The Nematode* Caenorhabditis elegans. Cold Spring Harbor, New York: Cold Spring Harbor Laboratory Press.